Exciton dynamics and device performance in polythiophene heterojunctions for photovoltaics

Stephanie V. Chasteen[*a], Sue A. Carter[a], Garry Rumbles[b]
[a]Physics Dept., University of California – Santa Cruz, 1156 High St., Santa Cruz, CA 95060
[b]Center for Basic Sciences, National Renewable Energy Lab., 1617 Cole Blvd., Golden, CO 80401

ABSTRACT

We present time-resolved photoluminescence studies in conjunction with device characterization of a variety of heterojunctions with poly-(3-hexylthiophene), or P3HT, as a means to understand how exciton dynamics affect device performance. We find that blends of P3HT with the electron-transporting polymer CN-ether-PPV and with the fullerene derivative PCBM result in ~4-fold and ~15-fold improvements in short-circuit currents, respectively, over neat-film P3HT on TiO_2 solgel. Despite efficient charge-transfer in P3HT:PCBM films, as evidenced by enhanced device performance and quenched steady-state luminescence, we observe only moderate reduction of the excited state lifetime, due to the already efficient non-radiative pathways in P3HT. We observe evidence for a new state that we assign to an exciplex in blends of P3HT with the electron-transporting polymer CN-ether-PPV. The exciplex state, which confirms the existence of charge-transfer between the two polymers, may account for the enhanced device performance of these blends by acting as a scavenger for excitons that would otherwise decay rapidly via non-radiative pathways. The long-range order of P3HT is disrupted when spin-cast on rough TiO_2 nanoparticles, and this results in a blueshift of the PL spectrum and a new long-lived decay component that we attribute to long-lived intrachain polarons. P3HT on smooth TiO_2 solgel films shows little or no quenching of the excited state, despite known charge transfer from P3HT to TiO_2.

Keywords: P3HT, PCBM, CN-ether-PPV, polymer solar cell, photovoltaic effect, conjugated polymers, fullerene, titanium dioxide, time-resolved photoluminescence, plastic electronics

1. INTRODUCTION

Heterojunctions of polythiophenes with a variety of electron-transporters (such as PCBM, metal oxides, and other conjugated polymers) have been widely studied as a means to improve the power conversion efficiencies of polymer photovoltaics. By providing multiple exciton dissociation sites, as well as separate charge transport pathways for electrons and holes, both charge generation and collection efficiency may be improved through the use of heterojunctions. P3HT has been considered a promising candidate for high-efficiency photovoltaics because of its semi-crystalline nature and tendency to form lamellar structures. This ordered morphology enhances charge transport and mobility, especially in regio-random versions of the polymer[1,2], and P3HT has field effect hole mobilities up to 0.1 $cm^2V^{-1}s^{-1}$, the highest yet observed[3]. The drawback of P3HT is high variability of the polymer purity and molecular weight, depending upon synthesis and purification techniques. P3HT on mesoporous TiO_2 films has yielded power efficiencies of ~0.45% under AM1.5[4]. P3HT has been successfully combined with CN-PPV, resulting in enhanced photocurrents and quenching of the photoluminescence of CN-PPV, indicating charge transfer between the two species[5]. P3HT:CdSe nanorod blends have achieved power efficiencies of 1.7% under AM1.5[6]. P3HT:PCBM devices have been well characterized and are known to have high photoluminescence quenching, and high short-circuit currents up to 8.5 mA/cm^2 and power efficiencies of 3.5%[7].

Time-resolved photoluminescence studies are a powerful way to examine exciton dynamics in thin films, giving insight into the mechanisms of exciton decay and charge-transfer. The simplest model (see below) suggests that upon excitation of a species X to X^*, that species may relax to form inter- or intra-chain excitons (A^*, B^*), which may decay radiatively or non-raditiavely, or interconvert. Each process is characterized by a rate constant *k*. Thus, in neat film one can expect to find at least two decay components, attributable to A^* and B^*.

*stephanie@physics.ucsc.edu; phone 831-459-4588; fax 831-459-3043; http://maxwell.ucsc.edu/~sacarter

Organic Photovoltaics VI, edited by Zakya H. Kafafi, Paul A. Lane,
Proc. of SPIE Vol. 5938, 59380J, (2005) · 0277-786X/05/$15 · doi: 10.1117/12.614243

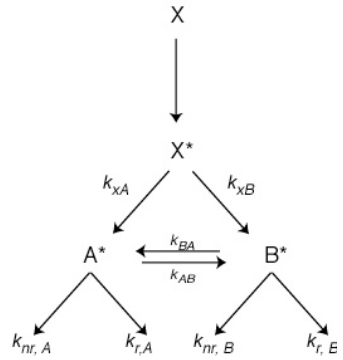

Charge-transfer to another material, such as PCBM, introduces a new, efficient rate constant which competes with these processes and, theoretically, reduces the overall decay time of the exciton. We combine device characterization on several P3HT heterojunctions with steady-state and time-resolved photoluminescence for additional insight into how these exciton dynamics affect device performance.

2. METHODOLOGY

We chose regio-regular poly-(3-hexylthiophene), or P3HT, as our hole-transporter. P3HT was purchased from Aldrich and purified using the Soxhlet procedure (first in hexane and then in chloroform) to obtain pure samples with a number-average MW ~20,000 as determined by GPC analysis. We used a variety of electron-transporting materials, including [6,6]-phenyl C61-butyric acid methyl ester, or PCBM (a soluble derivative of C_{60}; purchased from Nano-C), titanium dioxide solgel[8] (synthesized in our labs), titanium dioxide nanoparticles (~13 nm suspended in water; purchased from Solaronix) and the electron-transporting polymer CN-Ether-PPV[9]. CN-Ether-PPV is a derivative of the relatively insoluble CN-PPV and is designed to increase solubility and electron affinity relative to CN-PPV. Part of our work also includes the hole-transporter M3EH-PPV, which is an alternating copolymer of the well-characterized semiconducting polymer poly(2-methoxy-5-(2'-ethylhexyloxy)-1,4-phenylene-vinylene) or MEH-PPV. M3EH-PPV was synthesized by Horner reaction and has optical properties very similar to MEH-PPV[10]. Both M3EH-PPV and CN-ether-PPV were provided courtesy of H.-H. Hoerhold and H. Tillmann at the University of Jena in Germany. Organic structures are shown in Figure 1, below.

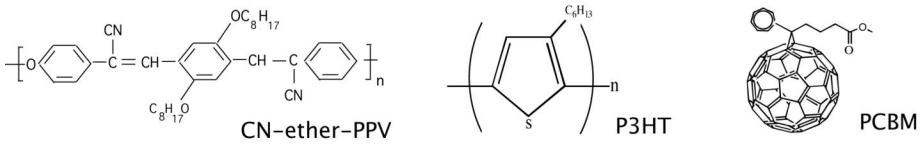

Figure 1. Polymer and material structures

TiO_2 solgel and nanoparticles are spin-cast and then annealed at 450°C for 1 hour. A transparent semiconductor, TiO_2 acts as an electron-transporter and hole-blocker due to its energy level structure. TiO_2 has been shown to improve device performance over bare ITO[8]. Devices are prepared and characterized as described elsewhere[11].

Current-density vs. voltage curves were measured using a 2400 Keithley source meter. Illumination is provided by a white light Xenon bulb with an output of approximately 80 mW/cm^2. Absorption spectra are taken on a Varian optical spectrometer. Thickness measurements are made using an atomic force microscope in contact mode and imaging is performed using a Nikon upright optical microscope with a transmission light source.

Steady state photoluminescence spectra were recorded using a Fluorolog-3 (JYHoriba) spectrometer that utilized a liquid N_2 cooled CCD detector. Monochromatic excitation light was generated by a Xenon arc lamp with double monochromator. Fluorescence was collected at 22° (45° for solutions) relative to the excitation beam, passed through a single monochromator containing a 300 line/mm grating and imaged on the liquid nitrogen-cooled CCD array. All PL

spectra were corrected for the spectral output of the excitation source and for the spectral response of the detection optics.

Fluorescence decay signals were measured using the technique of time correlated single photon counting (TCSPC)[12]. The spectrometer comprised a pulsed, picosecond diode laser (IBH NanoLED-10) operating at a wavelength of 438 nm and a repetition rate of 1 MHz. Emission was detected at 22° (45° for solutions) to excitation by focusing the emission onto the slits of a 0.25 m monochromator (SPEX mini mate) and subsequently detected by a photon counting photomultiplier tube (Hamamatsu H6279). The instrument response function (IRF) from this system when scattering the excitation light from a dilute solution of colloidal silica was determined to be 220 ps. Using a non-linear, least squares iterative deconvolution procedure[12] employing the Marquardt minimization routine, the influence of the IRF could be removed from the measured luminescence decay curves to reproduce the true decay kinetics with a temporal resolution of ~ 30 ps.

3. RESULTS

3.1 Device performance

J-V curves for the various device types are shown below in Figure 2. Neat film P3HT devices (on a TiO_2//Au structure) exhibit short circuit currents around 0.36 mA/cm^2 with a V_{oc} of 0.60 V and 42% FF, comparable to currents obtained in other studies[4]. Analogous structures on TiO_2 nanoparticles are expected to produce currents about twice as high, based on experiments on similar devices. P3HT devices on a PEDOT//Al architecture performed poorly (J_{sc} < 0.001 mA/cm^2, V_{oc} = 1.3 V) presumably because the transparent PEDOT cathode forces the poorly mobile electrons to cross the bulk from the P3HT/Al interface. Blends of P3HT with the electron-transporting polymer CN-ether-PPV had short-circuit currents up to 1.7 mA/cm^2 (V_{oc} = 0.94 V; FF = 24%). The fourfold improvement in current over neat film P3HT indicates efficient charge transfer from P3HT to CN-ether-PPV (and vice versa), as does the increase in V_{oc} due to the separation of electrons and holes to the HOMO of P3HT (~5.0 eV) and the LUMO of CN-ether-PPV (3.5 eV). The concomitant drop in FF suggests that charge transport is compromised in the blend. This may be due to the indirect charge pathways present in a phase-separated blend, or by high leakage in CN-ether-PPV, as suggested by the inability to fabricate a working photovoltaic from CN-ether-PPV alone as well as poor fill factors for other CN-ether-PPV blended devices. Unlike blends of M3EH-PPV:CN-ether-PPV, P3HT:CN-ether-PPV blends did not perform well on PEDOT//Al architecture, indicating that charge transport is not bipolar in the P3HT blends and performance is still severely limited by poor electron transport. Not surprisingly, 1:4 blends of P3HT:PCBM outperformed all other structures, with currents as high as 5.6 mA/cm^2 (V_{oc} = 0.63 V; FF = 34%). Power efficiencies range from ~ 0.1% (TiO_2/P3HT) to 1.5% (P3HT:PCBM).

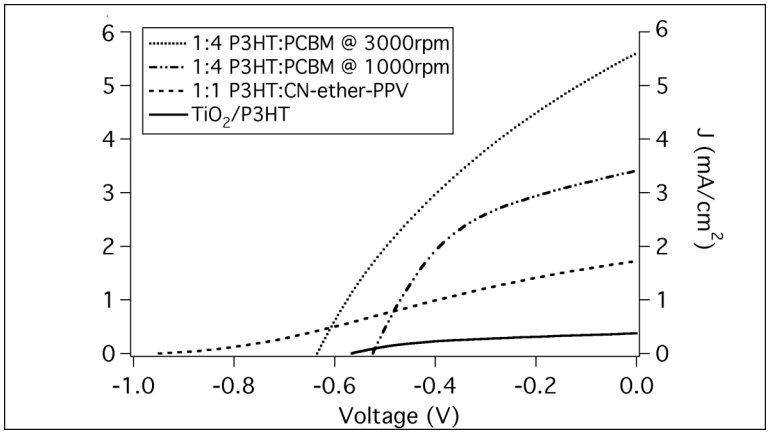

Figure 2. J-V curves for P3HT heterojunctions. Device thicknesses are 50-100 nm, except for the PCBM blend spun at 1000 rpm, which is 260 nm. All devices are on TiO_2 solgel//Au structure, except P3HT:PCBM devices, which are on PEDOT//Al structure and sourced negative so that all J-V curves appear in the same quadrant for ease of comparison.

P3HT and P3HT:CN-ether-PPV device performance is thickness-dependent, as expected for charge-transport limited devices. At first inspection, it appears that P3HT:PCBM devices are also thickness-dependent, but further examination reveals that morphological differences are responsible for differences in device performance. P3HT:PCBM devices are not expected to be thickness-dependent, based on previous findings that these devices are absorption-limited, not transport-limited, since device performance is positively correlated with thickness and not with temperature[13]. Devices spun at 3000 rpm performed better than those spun at 1000 rpm by a factor of 1.6, as can be seen in Figure 2 above. Though the devices differ in thickness (100 nm versus 260 nm), microscopic inspection of these films show morphological differences. As can be seen in Figure 3, below, aggregated features appear in P3HT:PCBM devices at all spin speeds, but they comprise a larger portion of the film at slower spin speeds (e.g., 1000 rpm; Figure 3A and 3B) than at faster spin speeds (e.g., 3000 rpm; figure 3C). In addition, for two films of equal film thickness (260 nm) but different morphologies (see Figure 3A and 3B), the device with fewer aggregated islands exhibits better performance. Thus, charge transport is most certainly hampered by the poor quality of films with more aggregated structures. We assume that these features are due to equilibrium processes which tend to be suppressed at higher spin speeds. An AFM image of one of the small features from the 4000 rpm film is shown in Figure 3C; it is about 20 um wide and 0.5 um tall. Similar star-like structures have been observed in 1:4 blends of P3HT-2.5 diyl with PCBM, becoming smaller at 1:1 blend ratios, suggesting that they can be attributed to crystallization of PCBM. In MDMO-PPV:PCBM blends, phase separation is observed starting at 1:1 blend ratios, with domains of pure PCBM formed in a polymer matrix at higher blend ratios, resulting in improved current densities for 1:4 blend ratios due to enhanced electron transport through the PCBM[14,15]. The same mechanism would appear to be at work in the present devices, with phase separation modulated by spin-speed rather than blend ratio. Some recent studies suggest that 1:1 ratios are thus more optimal for device performance[13,16]. Only 1:4 blend ratios were studied in the present work.

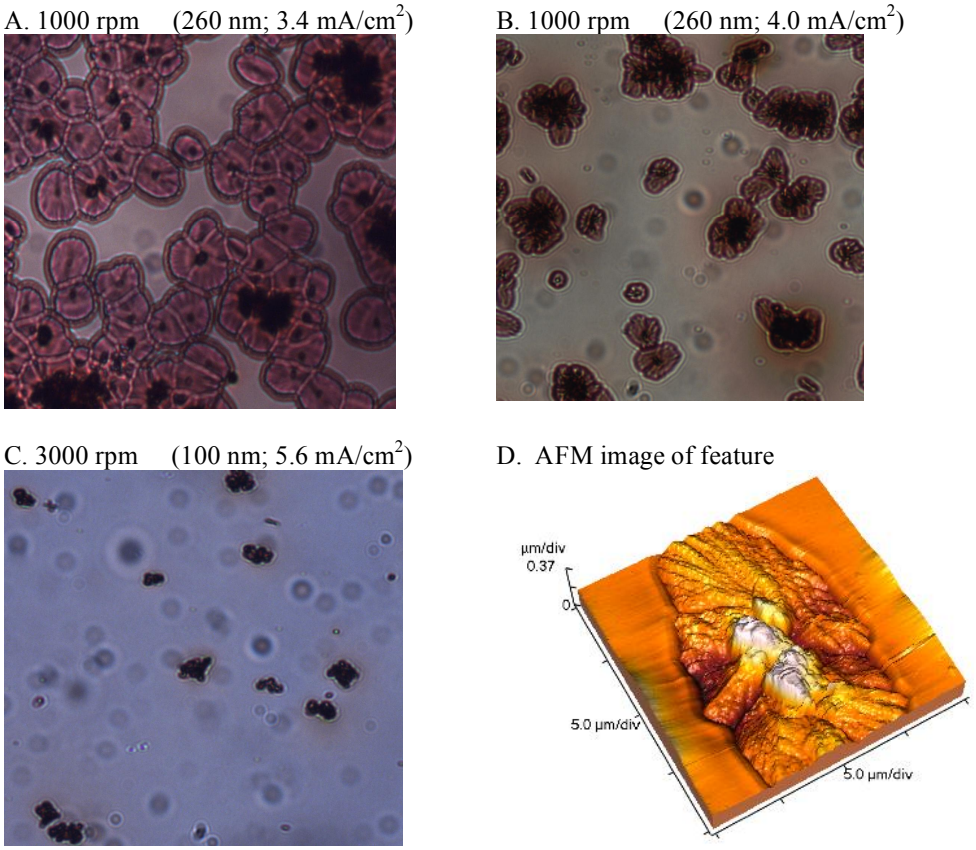

Figure 3. Optical images of 1:4 P3HT:PCBM mixtures spin-cast at [A] and [B] 1000 rpm (260 nm thick) and [C] 3000 rpm (100 nm thick). Images are 200 µm across. Surface features indicate increased aggregation with slower spin speed. Part [D] shows an AFM image of one of the smaller surface features, about 10 µm wide.

3.2 Steady-state spectroscopy

3.2.1 P3HT

Steady-state photoluminescence and absorption spectra of P3HT (solution, 30 nm film, and 100 nm film) are shown below in Figure 4A. P3HT films exhibit poor photoluminescence efficiency due to the high crystallinity in which radiative transitions are suppressed by strong interchain interactions[1]. All spectra, except for solution absorption, show clear vibronic structure. The broad absorption spectra of solution and film are characteristic of a distribution of conjugation lengths in the sample, in addition to a homogeneous broadening mechanism that arises from coupling between these segments[17,18]. Excited species in solution are contained within a 1D environment on isolated single chains, as opposed to a 3D environment within the strongly crystalline film structure, as evidenced by the strong redshift of both the absorption and PL spectra from solution to film. The 0-3' vibronic peak at 2.4 eV is less prominent in the absorption of thin (30 nm) films, which could be due to microcavity effects, a suppression of that transition in thin film, or an increase in the effective conjugation length due to high film crystallinity resulting in extended chains. The large Stokes loss from absorption to PL indicates that the excited state has a different conformation than the ground state. Absorption spectra of P3HT:CN-ether-PP blends (not shown) are well approximated by linear combinations of the neat polymers. The absorption and PL of CN-ether-PPV are shown, in comparison to P3HT film spectra, in Figure 4B. The two polymers are spectrally distinct.

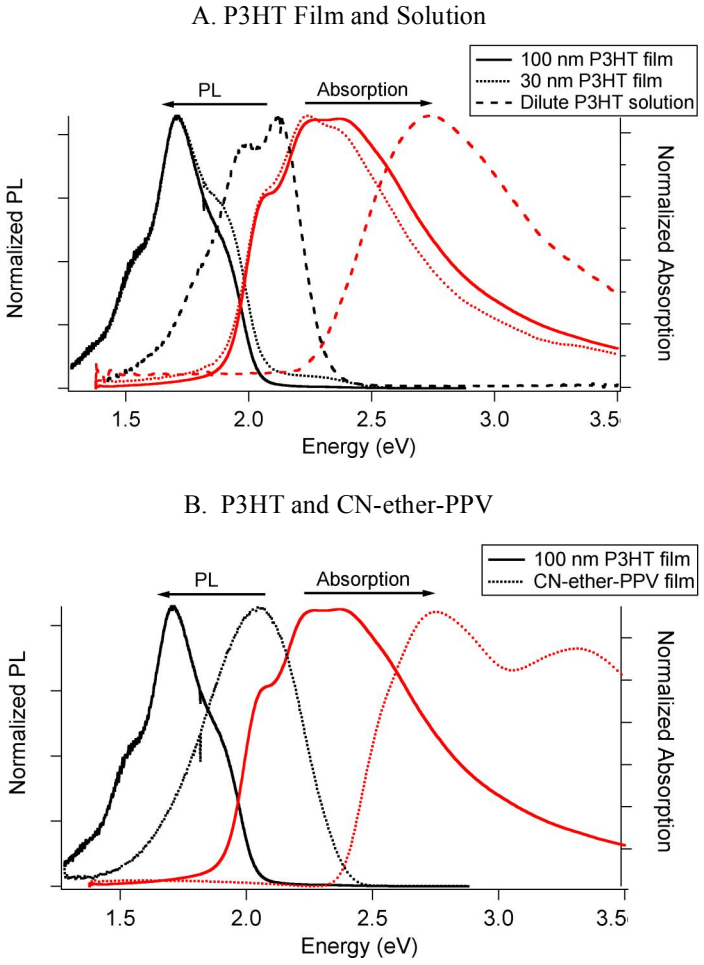

Figure 4. Steady-state absorption and photoluminescence spectra for [A] P3HT film and solution and [B] P3HT and CN-ether-PPV film. PL spectra are excited at 400 nm (3.1 eV) – on the blue edge of the absorption. The excitation energy had no observable effects upon the shape of the PL spectra. Vibronic structure in the absorption and PL spectra are indicative of interchain interactions.

3.2.2. P3HT:PCBM and P3HT:CN-ether-PPV blends

The magnitude of the photoluminescence of P3HT:PCBM and P3HT:CN-ether-PPV blends are well-quenched with respect to neat films. The relative photoluminescence measurements were obtained by comparing the intensity of the photoluminescence peaks for the films, corrected by the optical density at that excitaton wavelength. The error in these relative measurements is large, ± 20%, and all quenching proportions are well outside this margin of error. Quenching percentage is calculated by the difference in intensity between the neat film and the blend, normalized by the intensity of the neat film. At 1.7 eV emission, P3HT:PCBM films are quenched 99% relative to neat P3HT. At 2.0 eV emission, P3HT:CN-ether-PPV blends are quenched 96% relative to neat CN-ether-PPV.

The profile of the steady-state spectrum of P3HT:PCBM blends is not significantly different from that of neat P3HT, but the same is not true of blends of P3HT with CN-ether-PPV, as seen below in Figure 5, where a new PL feature at 1.85 eV is present. The spectrum of the blend contains spectral features at positions that are very similar to the neat P3HT films, where they are attributed to vibronic structure. It is difficult to understand how the blending of the two polymers can have such a dramatic impact on the profile, with an apparent reduction in the Huang-Rhys parameter, although an intensity distortion by re-absorption effects might suggest such an effect. However, the energetic difference between the HOMO of the hole-accepting P3HT and the LUMO of the electron-accepting CN-ether-PPV is 1.5 eV. The similarity between the HOMO/LUMO offset and the energy of this new peak suggests the presence of a new species formed by a complex between a hole (positive polaron) on P3HT and an electron (negative polaron) on CN-ether-PPV; i.e., an exciplex. The exciplex peak is present when both the P3HT and CN-ether-PPV are excited (2.5 eV), and also when predominantly CN-ether-PPV is excited (3.1 eV). Thus, excitation of CN-ether-PPV alone results in charge transfer to P3HT and formation of the exciplex. We cannot make a definitive statement regarding whether excitation of P3HT alone results in charge transfer to CN-ether-PPV. Note that there is significant overlap between the PL of CN-ether-PPV and the absorption of P3HT, suggesting that Förster energy transfer may occur from CN-ether-PPV to P3HT.

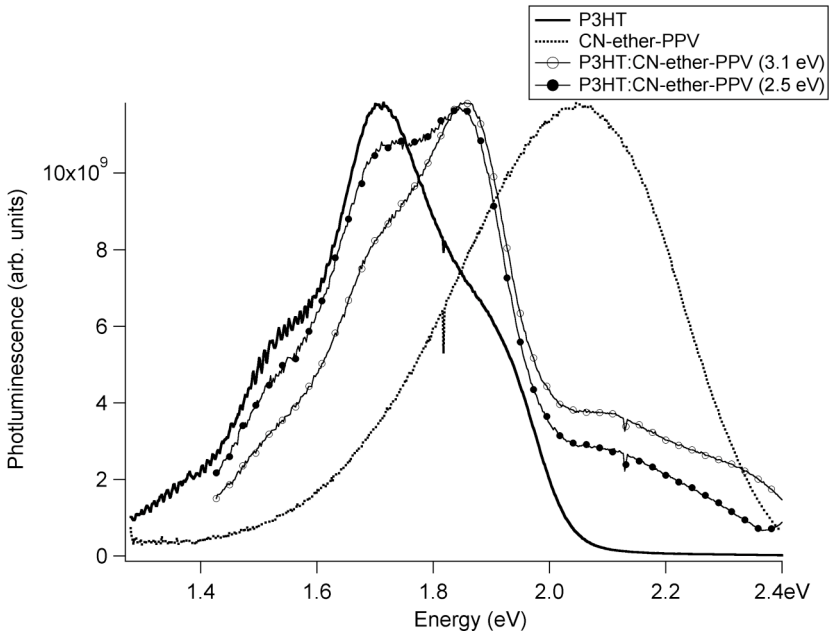

Figure 5. Steady-state photoluminescence spectra for P3HT, CN-ether-PPV, and a blend of the two. A new peak is present at 1.85 eV, which we attribute to an exciplex. The exciplex peak is present both at 2.5 eV excitation (P3HT and CN-ether-PPV) and 3.1 eV excitation (primarily CN-ether-PPV), and cannot be attributed to a linear combination of the neat polymers.

3.2.3 TiO_2/P3HT

Comparison of the photoluminescence intensity of films on nanoparticle and solgel layers poses a particular challenge, since the photoluminescence from the bulk film is likely to outweigh quenching effects at the interface, which may span only 5-10 nm. In an attempt to overcome this problem, thin, 30 nm films were deposited. All three films were deposited from the same solution at the same concentration and spin speed, resulting in similar film thicknesses. Results are shown below in Figure 6. The photoluminescence intensity is partially quenched by the solgel, but enhanced by the nanoparticle surface. Partial quenching by solgel is expected due to charge transfer to the solgel. The PL enhancement on the nanoparticles, as well as the shift of the photoluminescence peak towards the blue, is due to disruption of the crystalline order by the rough nanoparticle surface, suppressing interchain interactions and allowing additional radiative recombination. Such a blueshift has been previously observed in studies of P3HT infiltrated into mesoporous titania, which exhibit poor hole transport due to the disruption of pi-stacking in the polymer[4].

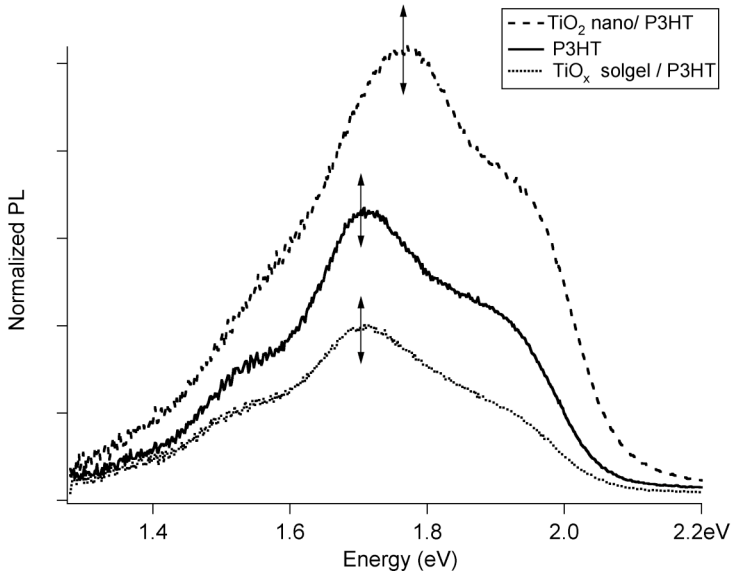

Figure 6. Relative steady-state photoluminescence at 3.1 eV excitation for 30 nm films of P3HT – neat film and deposited on TiO_2. P3HT on smooth solgel shows moderate quenching, whereas P3HT on rough nanoparticles shows some enhancement of the PL. Error bars represent 20% error in reproducibility of results.

3.3 Time-resolved photoluminescence

Photoluminescence decay curves were fit to a sum-of-exponential series, indicating the presence of multiple de-excitation pathways for charge carriers in these films. Decays are shown in Figure 7 (A and B) and primary decay components are reported in Table 1.

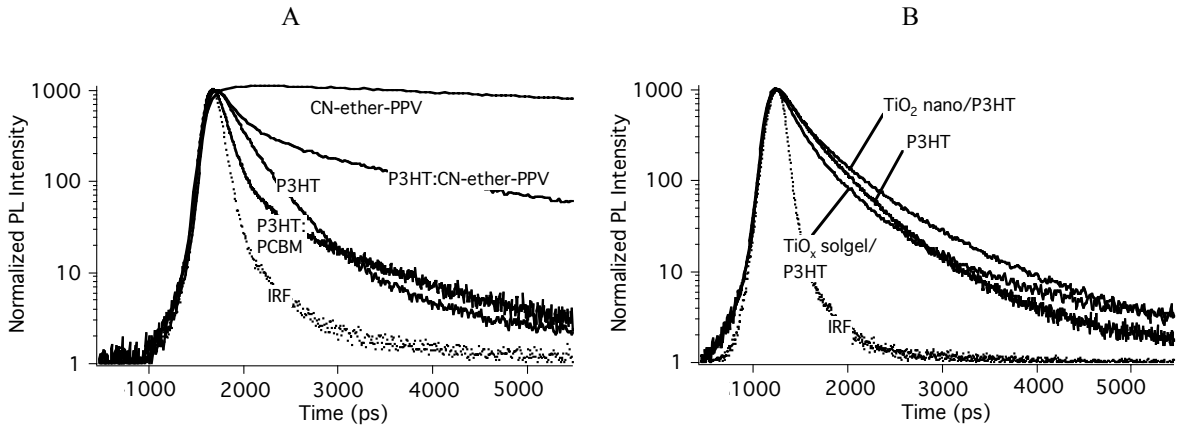

Figure 8. Time decays of P3HT blended (A) and layered (B) with different electron transporters, along with the instrument response function (IRF) for the apparatus. Films in (A) are thick (100-250 nm) w.r.t. the exciton diffusion length whereas films in (B) are thin (35-45 nm). All heterojunction decays contain long components that may be attributed to long-lived intrachain polaron states in P3HT due to disruption of the crystallinity and hence disorder in the film[1].

		T_1 (ns) ±0.01 ns	T_2 (ns) ±0.02 ns	T_3 (ns) ±0.02 ns	T_4 (ns) ±0.06 ns	T_5 (ns) ±0.13 ns	T_6 (ns) ±0.2 ns	Ave T
	P3HT solution			**0.54 (100%)**				0.54
Blends	100 nm P3HT	**0.11 (68%)**		0.51 (27%)				0.41
	CN-ether-PPV					6.2 (31%)	**13.9 (69%)**	11.6
	1:4 P3HT:PCBM	**0.09 (73%)**		0.45 (15%)				0.30
	1:1P3HT:CN-ether-PPV			0.44 (18%)	**2.1 (42%)**	6.4 (24%)		2.5
Layers	30 nm P3HT	0.05 (17%)	**0.26 (55%)**	0.60 (27%)				0.32
	TiO_2 nano/P3HT	0.10 (36%)	**0.36 (43%)**		0.91 (21%)			0.38
	TiO_x solgel/P3HT		**0.22 (68%)**	0.51 (27%)				0.34

Table 1. Time decay components from TCSPC analysis. Primary decay components are highlighted in bold for clarity and lifetimes are binned by short/medium/long for ease of comparison. All neat films are fit to 3 exponentials and blends are fit to 4 exponentials; decay components with less than 15% weight are not reported for clarity. Reduced chisquare for all fits is less than or equal to1.2 and Durbin-Watson parameter is greater than or equal to 1.7[12]. Average lifetime is calculated by weighting each time-component with its percentage yield. All emissions were detected at the PL peak of 1.78 eV, except for dilute solution, which was detected at 1.9 eV (the PL peak of solution).

3.3.1 P3HT

P3HT solutions decay with a characteristic lifetime of 0.54 ns, similar to previously published observations.[19,20] As stated previously, P3HT films and solution create drastically different environments for the excited state carriers, as evidenced by the difference in emission spectra; it is thus difficult to compare the decay times in film and solution, and we consider the similarity of T_2 in solution and film to be coincidental. Due to the strong vibronic structure and narrow emission spectrum in the steady-state, as well as the relatively short decay lifetimes, we take the excited state carriers to be intrachain excitons. The presence of multiple decay channels for intrachain excitons suggests that the simple model (light absorption results in creation of singlet excitons which decay via radiative and non-radiative channels) is incomplete. Excitons in different environments (for example, in the middle of a chain, the end of a chain, or a defect) may decay with different characteristic lifetimes.

Thick (100 nm) and thin (30 nm) films vary dramatically in their time decay. Both share a 27% yield of a medium length component, T_3 (0.51 – 0.60 ns), but the dominant component of thick P3HT is 0.11 ns (68%) whereas that of thin P3HT is 0.26 ns (55%). It is possible that long-range order is more easily developed in the thick films, enabling faster decay of T_1 due to enhanced pi-stacking. However, it is difficult to assign the components to inter- or intra- chain species with the current data.

3.3.2 P3HT:PCBM blend

The P3HT:PCBM blend appears only mildly quenched relative to P3HT. There is an increase in yield, and thus a greatly increased amplitude, for the short T_1 component, as well as a slight decrease in the longer T_3 component, indicating that there is efficient charge transfer from P3HT to PCBM. The sample used was spun at 2000 rpm and shows aggregated features as in Figure 3B. The long tail in the PL is due to a relatively high percentage yield (15%) of a medium-length component (1.2 ns, not reported in Table 1), which may be due delayed luminescence arising from the involvement of long-lived polaron states in P3HT[1].

3.3.3 P3HT:CN-ether-PPV blend

The photoluminescence decay profile of P3HT:CN-ether-PPV blends is well-quenched with respect to the long decay of CN-ether-PPV: The dominant 13.9 ns component of the CN-ether-PPV (which we assign to an interchain species due to the broad excimer-like PL spectrum of CN-ether-PPV) is completely absent in blends of P3HT:CN-ether-PPV. The absence of this emissive component can account, in part, for the efficient quenching of the CN-ether-PPV PL in the steady-state.

As can be seen in Figure 9, below, the average lifetime of the P3HT:CN-ether-PPV blends reaches a peak at 1.9 eV. This is due to an increase in the length and the % yield of the longer T_4 (2.1 ns in Table 1) and concomitant decrease in the shorter T_3 (0.44 ns in Table 1) around 1.9 eV, as illustrated in Figure 9, inset. Recalling the new peak in the steady-state emission at 1.85 eV, attributed to the exciplex, we assign T_4 (2.3 ns, 46% yield at 1.9 eV) to decay of the exciplex. T_3 is assigned to a delocalized excitonic species in P3HT neat film which transfers charge to the exciplex state. The slightly longer lifetime indicates that the exciplex state acts as a charge-trap state, perhaps resulting in a delayed luminescence.

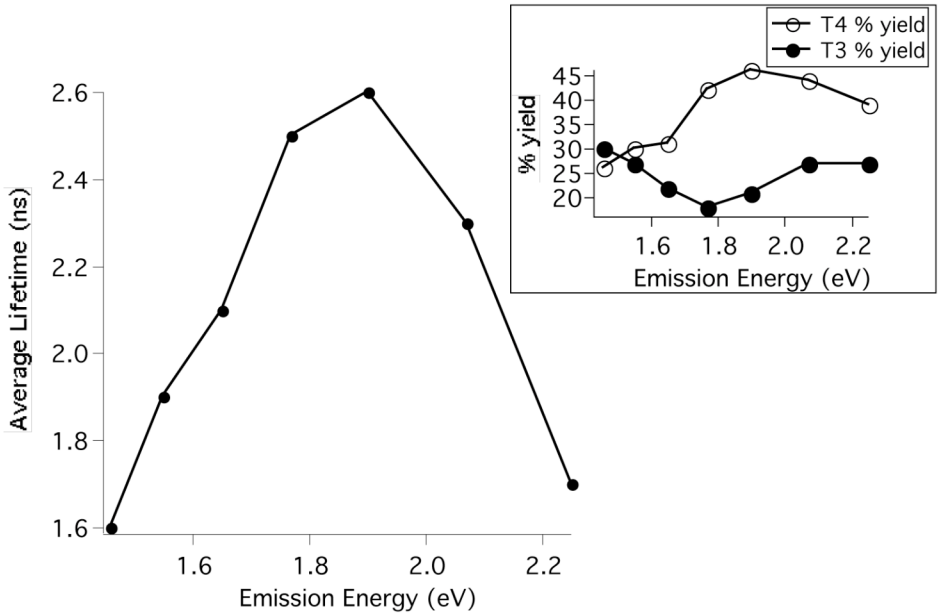

Figure 9. Average lifetime and % yields by emission energy for P3HT:CN-ether-PPV blends. The increase in lifetime at 1.9 eV, which is caused by an increase in the lifetime and yield of the long T_3 component, is attributed to exciplex emission at that energy.

3.3.4 TiO_2/P3HT heterojunctions

TiO_2/P3HT heterojunction films are ~ 30 nm thick and should be compared to 30 nm P3HT neat films. Both types of TiO_2/P3HT heterojunctions (smooth TiO_2 solgel and rough TiO_2 nanoparticles) appear surprisingly unquenched with respect to the decay of neat-film P3HT of similar thickness (~35 nm). The lack of quenching and absence of a new fast component due to charge transfer from P3HT to TiO_2 may be due to the dominance of the bulk emission over the quenching from the small interfacial area. A long decay component can be seen in the decay plots, and a new 0.91 ns component (21%) is present in TiO_2 nanoparticle/P3HT films. We attribute these long decay components to long-lived intrachain polaron states in P3HT which are enhanced in films on nanoparticle layers, which disrupt the crystalline pi-stacking. We note the striking similarity of TiO_2 solgel/P3HT decay components to those of 100 nm P3HT, which may be due to a poorly understood effect of the solgel upon P3HT morphology.

4. CONCLUSIONS

In conclusion, we performed device characterization, steady-state, and time-resolved spectroscopy measurements on a variety of heterojunctions of P3HT with electron transporting materials. We find that P3HT:CN-ether-PPV and P3HT:PCBM blends show enhanced currents over P3HT on TiO_2 solgel alone.

P3HT:PCBM devices show difference in aggregation depending upon spin-speed, such that lower spin-speeds result in increased aggregation at the expense of device performance. Aggregation of PCBM in the polymer matrix which may provide the best charge-transport structure at the cost of efficient charge separation. The decay times of P3HT:PCBM films are not drastically reduced compared to neat film P3HT due to the pre-existing efficient non-radiative pathways in P3HT. Thus, despite efficient charge-transfer from P3HT to PCBM, as evidenced by the quenching of the steady-state emission and enhanced device performance, the present study does not provide sufficient resolution in order to observe marked differences in the kinetics, unlike previous time-resolved infrared absorption studies [21].

We find evidence for an exciplex state between a positive polaron in P3HT (hole) and a negative polaron (electron) in CN-ether-PPV in P3HT:CN-ether-PPV blends. The exciplex is marked by a new photoluminescence peak at 1.9 eV in the steady-state, and a new 2.3 ns component which reaches a maximum yield, also at 1.9 eV. The exciplex is evidence of charge-transfer between the two polymers, which accounts for the quenching of the steady-state photoluminescence of CN-ether-PPV and enhanced device performance. The exciplex may also aid device performance by acting as a scavenger for excitons, which would otherwise decay via efficient non-radiative transfer.

Despite known charge transfer from P3HT to TiO_2 (due to the ability to create working photovoltaics on this structure), charge-transfer in the form of a short decay component is not observed in TiO_2 solgel/P3HT films. The time-decay appears longer-lived, which we attribute to long-lived polaron states in TiO_2. Thus, charge-transfer may correspond to longer, instead of shorter, decay times in time-resolved photoluminescence. TiO_2 nanoparticle layers disrupt the long-range order of P3HT, as evidenced by (a) a blueshift of the PL spectrum, indicating the shift from a 3D to 2D environment for excited carriers and (b) an enhancement of the steady-state PL, due to a decrease in non-radiative interchain carriers. Long-lived intrachain polaron states in this disorderd film are evidenced in a new 0.91 ns decay component.

For all polymer films, decay kinetics are complex and not well described by a simple model, in which a single excited state carrier, X*, relaxes to inter- and intra- chain species which may relax radiatively or non-radiatively. It is well-known that device characteristics are affected by morphology as well as quenching of the PL. A complete understanding of the kinetics of polymer films requires that we broaden our description of excited state carriers to include the environment that those carriers find themselves in – such as a crystalline or non-crystalline film, in the middle or end of a chain, or trapped at a kink or defect in the polymer. These variables are all likely to affect the excited state kinetics, and are difficult to control.

ACKNOWLEDGEMENTS

The authors would like to thank H.-H. Hörhold and H. Tillmann of the University of Jena, Germany, for providing the CN-ether-PPV.

S.V.C. thanks Marcus Jones of NREL for assisting with the analytical software for exponential fitting of the time-resolved data, and for assistance with the time-resolved and steady-state photoluminescence measurements at NREL. S.V.C. also thanks Sam Berweger of UCSC for fabrication of some of the devices.

S.A.C. acknowledges support from the Beyond the Horizons program of DOE-NREL, contract *ACQ-1-306-19-03*. S.V.C. acknowledges funding the same source for support and travel expenses necessary for this work.

REFERENCES

[1] X. M. Jiang, R. Osterbacka, C. P. An, and Z. V. Vardeny, Synth. Met. **137,** 1465-1468 (2003).
[2] M. Y. Song, J. K. Kim, K.-J. Kim, and K.-Y. Dong, Synth. Met. **137,** 1389-1390 (2003).
[3] H. Sirringhaus, N. Tessler, and R. H. Friend, Science **280,** 1741 (1998).
[4] K. M. Coakley and M. D. McGehee, Appl. Phys. Lett. **83,** 3380-3382 (2003).
[5] M. Onada, K. Tada, and K. Yoshino, IEICE Trans. Electron **E81-C,** 1051 (1998).
[6] W. U. Huynh, J. J. Dittmer, and A. P. Alivisatos, Science **295,** 2425-2427 (2002).
[7] F. Padinger, R. S. Rittberger, and N. S. Sariciftci, Advanced Functional Materials **13,** 85-88 (2003).
[8] A. C. Arango, L. R. Johnson, V. N. Bliznyuk, Z. Schlesinger, S. A. Carter, and H.-H. Horhold, Adv. Mater. **12,** 1689-1692 (2000).
[9] H. Tillmann and H.-H. Hörhold, Synth. Met. **101,** 138-139 (1999).
[10] S. Pfeiffer and H.-H. Hörhold, Macromol. Chem. Phys. **200,** 1870-1878 (1999).
[11] A. J. Breeze, Z. Schlesinger, P. J. Brock, and S. A. Carter, Phys. Rev. B **64,** 125205 (2001).
[12] D. V. O'Connor and D. Phillips, *Time-Correlated Single Photon Counting* (Academic Press, London, 1984).
[13] I. Riedel and V. Dyakonov, Phys. Stat. Sol. (a) **201,** 1332-1341 (2004).
[14] T. Martens, J. D'Haen, T. Munters, Z. Beelen, L. Goris, J. Manca, M. D'Olieslaeger, D. Vanderzande, L. De Schepper, and R. Andriessen, Synth. Met. **138,** 243 (2003).
[15] J. K. J. van Duren, X. Yang, J. Loos, C. W. T. Bulle-Liuwma, A. B. Sieval, J. C. Hummelen, and R. A. J. Janssen, Adv. Func. Mater. **14,** 425 (2004).
[16] Y. Kim, S. A. Choulis, J. Nelson, D. D. C. Bradley, S. Cook, and J. R. Durrant, Journal of Materials Science **40,** 1371-1376 (2005).
[17] G. D. Scholes, D. S. Larsen, G. R. Fleming, G. Rumbles, and P. L. Burn, Physical Review B **61,** 13670-13678 (2000).
[18] X. J. Yang, T. E. Dykstra, and G. D. Scholes, Physical Review B **71** (2005).
[19] L. Magnani, G. Rumbles, I. D. W. Samuel, K. Murray, S. C. Moratti, A. B. Holmes, and R. H. Friend, Synthetic Metals **84,** 899-900 (1997).
[20] G. Rumbles, I. D. W. Samuel, L. Magnani, K. A. Murray, A. J. DeMello, B. Crystall, S. C. Moratti, B. M. Stone, A. B. Holmes, and R. H. Friend, Synthetic Metals **76,** 47-51 (1996).
[21] S. C. J. Meskers, P. A. van Hal, A. J. H. Spiering, J. C. Hummelen, A. F. G. van der Meer, and R. A. J. Janssen, Physical Review B-Condensed Matter **61,** 9917-20 (2000).